Journal of the Korean Society of Marine Engineering, Vol.32, No.7, pp.1068~1079, 2008(ISSN 1226-9549)

A Tilt and Heading Estimation System for ROVs using Kalman Filters

Yun-Su Ha† and Thanh-Hoan Ngo*

(Received October 6, 2008 ; Revised November 19, 2008 ; Accepted November 25, 2008)

Abstract : Tilt and heading angles information of a remotely operated vehicle (ROV) are very important in underwater navigation. This paper presents a low cost tilt and heading estimation system. Three single axis rate gyros, a tri-axis accelerometer, and a tri-axis magnetometer are used. Output signals coming from these sensors are fused by two Kalman filters. The first Kalman filter is used to estimate roll and pitch angles and the other is for heading angle estimation. By using this method, we have obtained tilt (roll and pitch angles) and heading information which are reliable over long period of time. Results from experiments have shown the performance of the presented system.

Key words : Tilt estimation, Heading estimation, Kalman filter.

1. Introduction

Tilt and heading estimation is an important step in the design of an ROV since estimated angles are used in the lowest control loop to balance and navigate the vehicle. Commercially available products for this task provide good quality but tend to be expensive and heavy. In applications where budget is small like ours, developing a low cost tilt and heading estimation system while still providing high accuracy is necessary.

There are several kinds of sensor from which we can obtain tilt (roll and pitch) and heading information. For tilt measurement, following sensors are mostly used. The first is inclinometer. The sensor output is proportional to the tilt angle with respect to the field of gravity. This kind of sensor, however, has slow response and is affected by vibration, therefore, can't be used alone in tilt estimation system. The second is rate gyro sensor. The sensor measures the rate of rotation. To obtain angle of orientation, we have to integrate sensor signal. Thus, even small errors in the rate information can lead to drift in calculated angle. The third is accelerometer. The problem is that the sensor is sensitive to translational acceleration and should only be used for tilt measurement during phases of zero translational acceleration. For heading measurement, we can integrate gyro signal but it also lead to drift as in tilt measurement case. Another sensor can be used is magnetometer which measure magnetic field vector of the earth. Although the sensor itself has become very accurate and compact, magnetic field sensing is still very erroneous because of the existence of

† Corresponding Author(Division of Computer, Control and Electronic Communications Engineering, College of Engineering, Korea Maritime University, E-mail: hys@hhu.ac.kr. Tel:051-410-4347)
* Graduate School of Korea Maritime University

magnetic interferences.

To address the above problems, we need a fusion method to fuse signals coming from these kinds of sensor. In[1], Baerveldt and Klang have analyzed the problem of fusing inclinometers and gyros using linear complementary filter and frequency domain analysis. A similar filter has been recently used by Klaus Loffler et al in[2] for estimating tilt of a Biped robot. However, they only considered planar motions. Vaganay, Aldon, Fournier[3] proposed a tilt estimation system for a mobile robot using Extended Kalman filter to fuse data from accelerometers and gyroscopes. This method, however, requires that non gravitational acceleration has to be removed from the accelerometer output by using wheel encoder information. It is, therefore, inapplicable to ROV. Another Extended Kalman filter was presented by Barshan and Durrant-Whyte in[4],[5] where error model of gyroscope was constructed for estimating the heading angle of the robot. They showed that the error in heading estimation can be improved at least by factor of 5 if an adequate error model is supplied. Nevertheless, they found that additional information from some absolute sensing mechanism is necessary to overcome long-term drift. In[6], Ojeda and Borenstein introduced a new Fuzzy Logic Expert rule-based navigation method for fusing data from multiple low-to medium-cost gyroscopes and accelerometers in order to estimate the tilt and heading of a mobile robot. But encoder information is required to resolve the "standing and moving" ambiguity. More recently, in[7], Rehbinder and Hu developed a linear Kalman filter for sensing tilt angles. Their approach combines gyro and acceleration measurements when robot is under low acceleration state, and switches the filter rely mostly on the gyro signal when under high acceleration state. The filter has been successfully implemented on a walking robot; however, only tilt angles were estimated. Our approach combines the above filter and our proposed filter, consequently, not only tilt angles but also heading angle are estimated.

In our proposed method, two Kalman filter-based estimators have been used. The first one is based on the filter developed by Rehbinder and Hu and dedicates to tilt estimation. Results of the first one are used for tilt compensation of the earth's magnetic field vector measured by magnetometer. We then compensate for magnetic interferences that exist in the measured field vector by a calibration method and a proposed Kalman filter-based estimator. Finally, true North compensation is done to compensate for magnetic declination and we obtain heading angle with respect to geographic North pole. Tests have shown that we obtained tilt (roll and pitch angles) and heading information which are reliable over long period of time.

2. Theoretical background

2.1 Tilt and heading representation

Our aim is to estimate tilt and heading of the rigid body in the inertial space. To do this, three right-handed orthogonal coordinate frames are defined: navigation frame, n-frame, used as reference frame; the body frame, b-frame; and horizontal frame, h-frame. The n-frame has its origin at some point fixed in the body where the measurement system is located, and x_n-axis points North, y_n-axis points East, and z_n-axis points vertical down (to the Earth's centre). It is so called North-East-Down (NED) frame. The b-frame has the same origin as navigation frame's, the x_b-axis (roll) points forward, y_b-axis (pitch) points

to the right, and the z_b-axis (yaw) points downward. The b-frame is called the h-frame when their tilt angles are zeros. Various mathematical representations can be used to define the tilt and heading of a body frame with respect to a reference frame such as: direction cosine matrix, Euler angles, quaternions. In this work, Euler angle representation is utilized because of its intuitive nature and popularity despite drawback such as singularities. According to Euler's theorem, we can specify the orientation of the body frame relative to the reference frame by three angles (ψ,θ,ϕ), known as Euler angles, and obtained by three successive rotations about different axes, known as Euler angle sequence. Following Euler angle sequence is chosen to transform reference to body frame: rotate through angle ψ (yaw) about reference z-axis, rotate through angle θ (pitch) about new y-axis, rotate through angle ϕ (roll) about new x-axis. The three rotations may be expressed mathematically by following three separate direction cosine matrices, respectively:

$$\boldsymbol{C}_z = \begin{bmatrix} \cos\psi & \sin\psi & 0 \\ -\sin\psi & \cos\psi & 0 \\ 0 & 0 & 1 \end{bmatrix} \tag{1}$$

$$\boldsymbol{C}_y = \begin{bmatrix} \cos\theta & 0 & -\sin\theta \\ 0 & 1 & 0 \\ \sin\theta & 0 & \cos\theta \end{bmatrix} \tag{2}$$

$$\boldsymbol{C}_x = \begin{bmatrix} 1 & 0 & 0 \\ 0 & \cos\phi & \sin\phi \\ 0 & -\sin\phi & \cos\phi \end{bmatrix} \tag{3}$$

Thus, a transformation from reference to body axes may be expressed as product of these three separate transformations as follows:

where $\mathrm{c}\psi = \cos\psi$, etc.

Similarly, the inverse transformation from body to reference axes is given by:

$$\boldsymbol{C}_n^b = \boldsymbol{C}_x\boldsymbol{C}_y\boldsymbol{C}_z = \begin{bmatrix} \mathrm{c}\psi\mathrm{c}\theta & \mathrm{s}\psi\mathrm{c}\theta & -\mathrm{s}\theta \\ -\mathrm{s}\psi\mathrm{c}\phi+\mathrm{c}\psi\mathrm{s}\theta\mathrm{s}\phi & \mathrm{c}\psi\mathrm{c}\phi+\mathrm{s}\psi\mathrm{s}\theta\mathrm{s}\phi & \mathrm{c}\theta\mathrm{s}\phi \\ \mathrm{s}\psi\mathrm{s}\phi+\mathrm{c}\psi\mathrm{s}\theta\mathrm{c}\phi & \mathrm{s}\psi\mathrm{s}\theta\mathrm{c}\phi-\mathrm{c}\psi\mathrm{s}\phi & \mathrm{c}\theta\mathrm{c}\phi \end{bmatrix} \tag{4}$$

$$\boldsymbol{C}_b^n = \left(\boldsymbol{C}_n^b\right)^T = \left(\boldsymbol{C}_z\right)^T\left(\boldsymbol{C}_y\right)^T\left(\boldsymbol{C}_x\right)^T \tag{5}$$

2.2 Tilt and heading determination using rate gyro

Rates of rotation of the body frame relative to the reference frame can be expressed in terms of the derivatives of the Euler angles, $(\dot{\psi},\dot{\theta},\dot{\phi})$, called "Euler rates". Specifically, Euler rates and rate gyros are related by[8]:

$$\begin{bmatrix} \dot{\phi} \\ \dot{\theta} \\ \dot{\psi} \end{bmatrix} = \begin{bmatrix} 1 & \sin\phi\tan\theta & \cos\phi\tan\theta \\ 0 & \cos\phi & -\sin\phi \\ 0 & \dfrac{\sin\phi}{\cos\theta} & \dfrac{\cos\phi}{\cos\theta} \end{bmatrix} \begin{bmatrix} \omega_x \\ \omega_y \\ \omega_z \end{bmatrix} \tag{6}$$

where ω_x, ω_y, and ω_z are the rates of rotation of the body around the respective axes of the body frame and are measured using rate gyros. If initial Euler angles and rate gyros data are known, we can calculate Euler angles by solving (6) using numerical integration. However, as mentioned above, there always exist errors in rate gyros such as axis misalignment, fixed bias, drift bias, and so on. These errors cause the integration result to drift from the true values as a function of time.

2.3 Tilt determination using accelerometer

Since the accelerometer in this application is fixed to the body, it provides a measurement of specific force in the b-frame, denoted $\boldsymbol{f}_b=[f_{xb}\ f_{yb}\ f_{zb}]^T$. We have[8]:

$$\boldsymbol{f}_b = \boldsymbol{C}_n^b\left(\boldsymbol{a}_n - \boldsymbol{g}^n\right) \tag{7}$$

where $\boldsymbol{a}_n=[a_{xn}\ a_{yn}\ a_{zn}]^T$ is the acceleration of the body in the n-frame and $\boldsymbol{g}^n=[0\ 0\ g]^T$ is the mass attraction gravitation vector with g=9.81 m/s^2.

Denote $\boldsymbol{x}$ is the third column of $\boldsymbol{C}_n^b$, rearranging (7), we have:

$$\boldsymbol{f}_b = \boldsymbol{C}_n^b \boldsymbol{a}_n - \boldsymbol{x}g \tag{8}$$

When the body is not accelerating, $\boldsymbol{a}_n$=0, we can write:

$$\boldsymbol{f}_b = -\boldsymbol{x}g \tag{9}$$

From (9), tilt angles are calculated as:

$$\theta_{ACC} = \sin^{-1}\left(\frac{f_{xb}}{g}\right), \phi_{ACC} = \sin^{-1}\left(\frac{-f_{yb}}{g\cos\theta}\right) \tag{10}$$

It should be noted that the tilt determination using (10) is true only if the body is not accelerating. When the body is accelerating or vibrating, tilt angles calculated from accelerometer measurements are erroneous.

2.4 Heading determination using magnetometer

To determine heading angle of the system from earth's magnetic field vector measurement, we have to know components of the vector in h-frame, denoted $\boldsymbol{m}_h=[m_{xh}\ m_{yh}\ m_{zh}]^T$ as illustrated in Fig. 1.

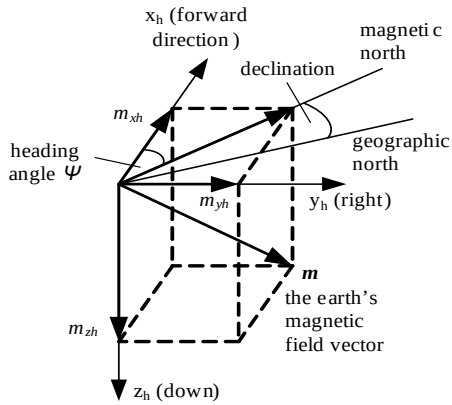

Fig. 1 Identify heading angle by measuring components of the earth's magnetic field vector

The heading angle ψ is calculated as follows:

$$\psi_{MAG} = arctg\left(-\frac{m_{yh}}{m_{xh}}\right) \tag{11}$$

However, in our application, the magnetometer is fixed to the vehicle's body, it provides a measurement of earth's magnetic field vector in the b-frame, denoted $\boldsymbol{m}_b=[m_{xb}\ m_{yb}\ m_{zb}]^T$. Hence the measured vector has to be transformed from b-frame into h-frame by applying the rotational equations shown below[9]:

$$\begin{bmatrix} m_{xh} \\ m_{yh} \\ m_{zh} \end{bmatrix} = \begin{bmatrix} \cos\theta & \sin\phi\sin\theta & \cos\phi\sin\theta \\ 0 & \cos\phi & -\sin\phi \\ -\sin\theta & \sin\phi\cos\theta & \cos\phi\cos\theta \end{bmatrix} \begin{bmatrix} m_{xb} \\ m_{yb} \\ m_{zb} \end{bmatrix} \tag{12}$$

where ϕ and θ are tilt angles (roll and pitch) of the vehicle's body. This technique is often referred to as tilt compensation or electronically gimbaling. In previous works[10],[11], tilt angles which are used for tilt compensation is determined by using accelerometer measurements.

As mentioned above, this method has good performance when the body is static but turns to be very erroneous when the body is accelerating or vibrating. The error in tilt angles measurement would result in tilt compensation errors, consequently, heading angle error. Another problem of determining heading angle using magnetometer data is the existence of magnetic interferences. When the sensor works in an open area in the area in the absence of any magnetic interference there is no distortion affects on the earth's magnetic field and the calculated heading angle is correct. In reality, though, the magnetometer is mounted in the vehicle where vehicle's platform and onboard components such as the motors, electric cables, etc. produce magnetic interferences. In addition, there are magnetic interferences produced by external objects such as passing vehicles, buildings, high-voltage wires, transformers, large metal structures, etc. These interferences will distort, or bend, the earth's field which will result in heading angle error. Compensating for error due to magnetic

interferences is not a trivial task.

3. Design tilt and heading estimation system

Each method presented in previous section has advantages and disadvantages. Method using rate gyro has good performance in short time but results in drift after long period. Meanwhile, method using accelerometer has good performance when the body is under non-acceleration state but is erroneous when the body is accelerating or vibrating. Method using magnetometer has no drift but is correct only in the absence of magnetic interference. Therefore, a fusion method is necessary to exploit advantages of each method. A proposed fusion method will be presented in following section.

3.1 Hardware design

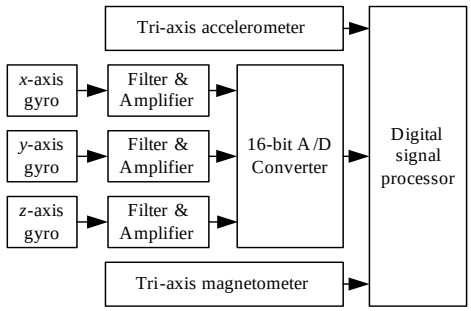

Fig. 2 Tilt and heading estimation system block schematic

In our approach, three single-axis rate gyros, a tri-axis accelerometer, and a tri-axis magnetometer are used(Fig.2).

Rate gyro adopted is low-cost single-axis ENC-03M manufactured by Murata. The maximum angular velocity that can be measured is +/-300 deg/sec. Sensor outputs are connected to high-pass filters and low-pass filters to reduce the effect of temperature drift and suppress output noise.

For acceleration measurement, digital output tri-axis accelerometer LIS3LV02DQ is used. It has a user selectable full scale of +/-2g, +/-6g and is capable of measuring acceleration over a bandwidth of 640Hz for all axes. With I2C/SPI serial interface, the sensor can be connected directly to processing unit without any signal conditioning circuit.

Magnetometer adopted is tri-axis magnetometer MicroMag3. The MicroMag3 combines PNI Corporation's patented Magneto-Inductive sensors and provides measurement of components of the earth's field vector on three axes of right-handed orthogonal coordinate. The SPI interface allows easy access to the sensor measurement parameters and magnetic field measurement data.

Sensor data are sent to digital signal controller TMS320F2812 where data fusion algorithm is implemented.

3.2 Data fusion algorithm

Sensor's signals are blended by two Kalman filter-based estimators. The tilt estimator which is based on[7] estimates tilt angles by fusing rate gyro and accelerometer data. To estimate heading angle, we propose the heading estimator where rate gyro and magnetometer data are fused. Note that output of the tilt estimator is used by the heading estimator for tilt compensation of magnetometer data. Whole system is illustrated in Fig. 3.

3.2.1 Tilt estimation

The direction cosine matrix C_b^n may be calculated from angular measurements provided by the rate gyros using following equation[8]:

$$\dot{C}_b^n = C_b^n \Omega \tag{13}$$

where Ω is the skew matrix

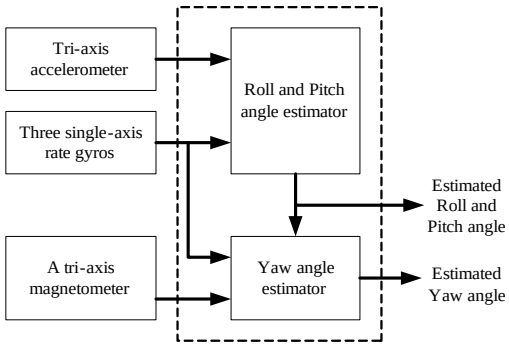

Fig. 3 Data fusion algorithm

$$\Omega = \begin{pmatrix} 0 & -\omega_z & \omega_y \\ \omega_z & 0 & -\omega_x \\ -\omega_y & \omega_x & 0 \end{pmatrix}$$

which is formed from the vector ω=[ω_x ω_y ω_z]^T. From (13), direction cosine matrix C_n^b may be calculated from:

$$\dot{C}_n^b = \left(\dot{C}_b^n\right)^T = (\Omega)^T \left(C_b^n\right)^T = (\Omega)^T C_n^b \tag{14}$$

Note that the third column of C_n^b is independent of yaw and that if that column could be estimated, then it would be possible to extract pitch and roll from it[7]. Denote x is the third column of C_n^b, from (14) we have:

$$\dot{x} = (\Omega)^T x \tag{15}$$

For notational simplicity, we redefine $S(\omega)=(\Omega)^T$ and have following equation:

$$\dot{x} = S(\omega) x \tag{16}$$

Note that $||x||=1$ due to that x is a column of a rotation matrix and thus has to be of unit length. Denote h is sample time and assume that the turn rate vector $\omega(t)=\omega_k=[\omega_{kx} \ \omega_{ky} \ \omega_{kz}]^T$ for $t \in [kh, kh+h)$ then we have the discrete time model:

$$x_k = \Phi_k x_{k-1} \tag{17}$$

where $\Phi_k = e^{S(\omega_k)h}$ has a closed form solution given by $\Phi_k = I + a_1 S(\omega_k) h + a_2 \left(S(\omega_k) h\right)^2$ [8] with

$$a_1 = 1 - \frac{\left(\|\omega_k\| h\right)^2}{3!} + \frac{\left(\|\omega_k\| h\right)^4}{5!} - \ldots$$

$$a_2 = \frac{1}{2!} - \frac{\left(\|\omega_k\| h\right)^2}{4!} + \frac{\left(\|\omega_k\| h\right)^4}{6!} - \ldots$$

Consider x as state vector and introduce a process noise w incorporating inaccuracies in modeling and gyro noise, the state transition equation is:

$$x_k = \Phi_k x_{k-1} + w_k \tag{18}$$

where w_k is presumed uncorrelated, zero-mean, and Gaussian with constant variance Q_k.

A. Estimation under non-acceleration

Consider accelerometer measurement f_b=[f_{xb} f_{yb} f_{zb}]^T as measurement vector z. When the accelerations are so low that we can consider as zero, from (9), the measurement equation can be written:

$$z_k = -x_k g + v_k \Leftrightarrow z_k = H x_k + v_k \tag{19}$$

where v_k is the measurement noise vector which models accelerometers noise as well as high-frequency accelerations. v_k is presumed uncorrelated, zero-mean, and Gaussian with constant R_k. And $H = -gI_3$ is measurement matrix. The resultant Kalman-filtering equation is given by:

$$\hat{x}_k = \Phi_k \hat{x}_{k-1} + K_k \left(z_k - H \Phi_k \hat{x}_{k-1}\right) \tag{20}$$

where K_k represents the Kalman gain matrix and are computed from the matrix Riccati equations given by[12]:

$$\begin{aligned}\boldsymbol{M}_k &= \boldsymbol{\Phi}_k \boldsymbol{P}_{k-1}\boldsymbol{\Phi}_k^T + \boldsymbol{Q}_k \\ \boldsymbol{K}_k &= \boldsymbol{M}_k \boldsymbol{H}^T \left(\boldsymbol{H}\boldsymbol{M}_k \boldsymbol{H}^T + \boldsymbol{R}_k\right)^{-1} \\ \boldsymbol{P}_k &= (\boldsymbol{I} - \boldsymbol{K}_k \boldsymbol{H})\boldsymbol{M}_k\end{aligned} \tag{21}$$

The estimated state vector $\hat{\boldsymbol{x}}_k$ is not of unit length. To guarantee the constraint $||\boldsymbol{x}||=1$ as mentioned above, we can write[7]:

$$\hat{\boldsymbol{x}}_k = \begin{cases} \hat{\boldsymbol{x}}_k / \left\|\hat{\boldsymbol{x}}_k\right\| \text{ if } \hat{\boldsymbol{x}}_k \neq 0, \\ \hat{\boldsymbol{x}}_{k-1} \quad \text{if } \hat{\boldsymbol{x}}_k = 0. \end{cases} \tag{22}$$

B. Estimation under acceleration

When the system is under acceleration, the measurement noise $\boldsymbol{v}_k$ is large and we can set the measurement noise covariance matrix $\boldsymbol{R}_k$ to infinity. Therefore, Kalman gain matrix $\boldsymbol{K}_k$=0 and state vector is estimated as:

$$\hat{\boldsymbol{x}}_k = \boldsymbol{\Phi}_k \hat{\boldsymbol{x}}_{k-1} \tag{23}$$

It means that when the system is under acceleration, tilt estimation is only based on rate gyros data. The same as non-acceleration case, the estimated state vector is modified by (22).

C. Acceleration detection

The problem is how to detect acceleration or rather, to detect non-acceleration. Recall that the accelerometer model is $\boldsymbol{f}_b = \boldsymbol{C}_n^b \boldsymbol{a}_n - \boldsymbol{x}g$. At non-acceleration state, $\boldsymbol{a}_n = 0$ and $\boldsymbol{f}_b = -\boldsymbol{x}g$, therefore, we have:

$$\left\|\boldsymbol{f}_b\right\| = g\left\|\boldsymbol{x}\right\| = g \tag{24}$$

It means that at non-accelerations state, the specific force $\boldsymbol{f}_b$ is moving on the sphere with radius of 1g. This condition must hold for certain amount of time before the system is considered under non- acceleration state[7].

D. Tilt calculation

As defined above, the state vector $\boldsymbol{x}$ is the third column of rotation matrix $\boldsymbol{C}_n^b$, hence $\boldsymbol{x} = [-\sin\theta \;\; \cos\theta\sin\phi \;\; \cos\theta\cos\phi]^T$. From the estimated state vector $\hat{\boldsymbol{x}}_k = [\hat{x}_{k1} \; \hat{x}_{k2} \; \hat{x}_{k3}]^T$, we can estimate tilt as:

$$\hat{\theta}_k = \arcsin\left(-\hat{x}_{k1}\right), \hat{\phi}_k = \arcsin\left(\frac{\hat{x}_{k2}}{\cos\hat{\theta}_k}\right) \tag{25}$$

3.2.2 Heading estimation

To estimate heading angle from magnetometer data, we need to reduce tilt compensation error and to compensate for magnetic interferences. To reduce tilt compensation error, we propose to use tilt angles which are provided by the tilt estimator for tilt compensation. By using this estimator, tilt angles measurement errors are small even when the body is accelerating or vibrating. Consequently, tilt compensation error is reduced. To compensate for magnetic interferences, we classified them into two kinds: deterministic magnetic interference and non-deterministic magnetic interference. Compensation method for error due to each kind of interferences will be presented.

A. Deterministic magnetic interference compensation

Deterministic interference means that the interference source is at a fixed position relative to the magnetic sensor and that its magnitude is constant versus time. The influence of deterministic interference on a magnetometer can be assessed by inspection of a test diagram shown in Fig.4. The diagram is a Lissajous figure, yielded by a 360^0 rotation of the magnetometer in a horizontal plane and recording of the magnetometer output signals Y versus X. Without any magnetic interference, the diagram appears as a circle, having its centre at (0,0) and a radius equal to the magnitude of the earth field. All

interference effects appear as a deviation from this shape. There are two different kinds of deterministic interference can occur, called “hard iron interference” and “soft iron interference”.

Hard iron interference is caused by the presence of anything that acts like a magnet. It could be a magnet or it could be things have some residual magnetic field. These could be things like screwdrivers which intentionally magnetized or things like the sheet metal of an automobile which is not really intended to be magnetized but in the manufacturing process does tend to get magnetized. These cause a magnetic field in the local area, which is vectorially added to the earth field. Thus, in the test diagram this effect appears as a shift of the circle's centre to (Xoff, Yoff) where Xoff and Yoff are the components of the interference field.

Soft iron interference occurs due to the presence of ferromagnetic materials. In this case the earth field will be distorted. Steel is the primary material that's going to do this, although there are some other materials out there that are ferromagnetic. Basically anything that a magnetic would stick to is a ferromagnetic material. The effect of soft iron interference is dependent on heading angle. Therefore, it appears as a deformation of the circle (slightly ellipsoid) in the test diagram.

To compensate for deterministic magnetic interference, compensation method presented in[13] has been used. Two scale factors Xsf and Ysf has been determined to change the ellipsoid response to a circle while offset values Xoff and Yoff to center the circle around the (0,0) origin.

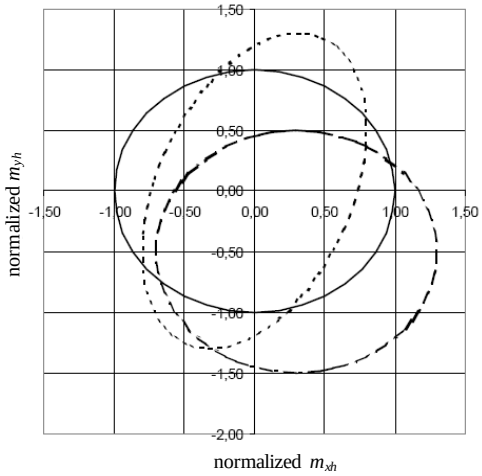

Fig. 4 Effect of hard iron and soft iron interference. Solid line denotes no interference, dashed dot line hard iron effect, and dot line soft iron effect

B. Non-deterministic magnetic interference compensation

Besides deterministic magnetic interference which can be compensated, there is non-deterministic magnetic interference. Its source is not at a fixed position relative to the magnetic sensor and/or that its magnitude is change versus time. It can be caused, for instance, by passing vehicles or nearby large metal structures such as buildings. Because of non-deterministic characteristic, this interference cannot be compensated easily. In this work, we proposed to fuse magnetometer data with rate gyro data by a Kalman filter. From (6), we have:

$$\dot{\psi} = \frac{\sin\phi}{\cos\theta}\omega_y + \frac{\cos\phi}{\cos\theta}\omega_z \tag{26}$$

Consider ψ as state variable, x, and introduce a process noise w incorporating inaccuracies in modeling and gyro noise, the state transition equation is:

$$x_k = x_{k-1} + \boldsymbol{G}_k \boldsymbol{u}_{k-1} + w_k \tag{27}$$

where

$$\boldsymbol{G}_k = \begin{bmatrix} \sin\phi & \cos\phi \\ \cos\theta & \cos\theta \end{bmatrix}, \boldsymbol{u}_k = \begin{bmatrix} \omega_{ky} & \omega_{kz} \end{bmatrix}^T \times h$$

with h is sample time and w_k has variance Q_k. Note that ϕ and θ has been estimated by tilt estimator.

From magnetometer measurement, $\boldsymbol{m}_b$, solve (11) and (12), we have heading angle ψ_{MAG}. Consider ψ_{MAG} as measurement variable, z, and introduce a measurement noise v which models the magnetic sensor noise, the measurement equation is:

$$z_k = x_k + v_k \tag{28}$$

with v_k has variance r_k. The resultant Kalman-filtering equation is given by:

$$\hat{x}_k = \hat{x}_{k-1} + \boldsymbol{G}_k \boldsymbol{u}_{k-1} + k_k \left(z_k - \hat{x}_{k-1} - \boldsymbol{G}_k \boldsymbol{u}_{k-1} \right) \tag{29}$$

where k_k represents the Kalman gain and are given by:

$$\begin{aligned} m_k &= p_{k-1} + q_k \\ k_k &= m_k \left(m_k + r_k \right)^{-1} \\ p_k &= (1 - k_k) m_k \end{aligned} \tag{30}$$

When the magnetometer is affected by non-deterministic magnetic interference, magnetometer data are invalid and we can set the measurement noise variance r_k to infinity. Therefore, Kalman gain matrix k_k=0 and state vector is estimated as:

$$\hat{x}_k = \hat{x}_{k-1} + \boldsymbol{G}_k \boldsymbol{u}_{k-1} \tag{31}$$

It means that when non-deterministic magnetic interference exists, heading estimation is only based on rate gyro data.

The problem is how to detect non-deterministic magnetic interference exists or not. It is based on the deviation of the magnetic field norm and the dip angle which are calculated from magnetometer data. If the measured magnetic vector lies on the sphere with the normalized radius of 1 and the calculated magnetic field inclination is correct then earth's magnetic field is considered as homogeneous and non-deterministic magnetic interference doesn't exist[14]. From estimated state variable $\hat{x}_k$, the estimated heading angle is:

$$\hat{\psi}_k = \hat{x}_k \tag{32}$$

C. True North compensation

After compensating for tilt, deterministic and non-deterministic magnetic interference, we obtain heading angle with respect to magnetic North pole. However, there is angular difference between magnetic North pole and geographic North pole. This angle difference, which varies over the earth's surface, is called the magnetic declination and can be elimated by using compensation table based on the World Magnetic Model. Finally, we obtain heading angle with respect to geographic North pole.

4. Experiments

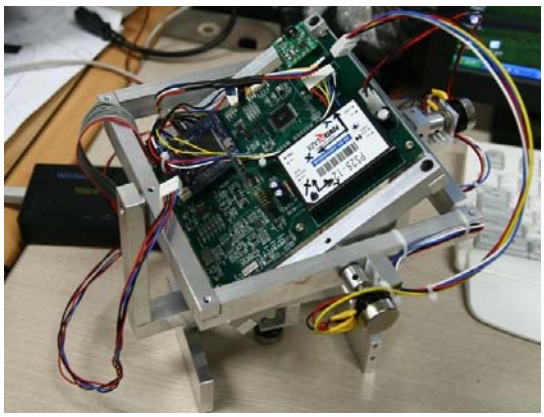

Fig. 5 The heading estimation system on three axes gimbal structure.

The tilt and heading estimation system is installed on three axes gimbal structure where true tilt and heading angles of the system can be measured by using potentiometers as illustrated in Fig. 5. Estimated and true angles are sent to PC through COM port for performance verification.

To compare performance of the tilt estimator used in our work and tilt measurement approach used in previous works (where accelerometer has been used), two experiments has been done. In first experiment, the gimbal structure doesn't move (no translational acceleration exists) and the system's tilt angles are changed manually. Tilt angles calculated by two approaches are shown in Fig. 6. From this figure, it can be drawn that the tilt estimator and accelerometer have the same performance in tilt measurement when no translational exists.

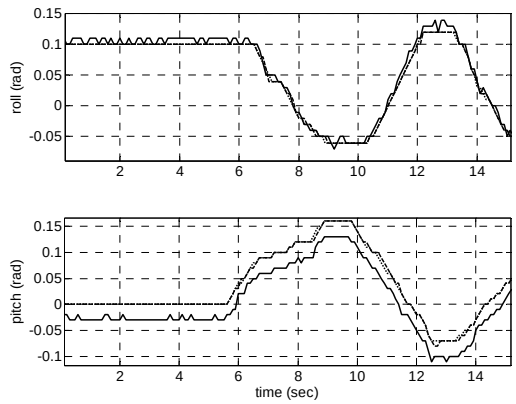

Fig. 6 Tilt angles (roll and pitch) when no translational acceleration exists. Solid lines denote true angles, dashed lines angles calculated from accelerometer measurements, and dot lines estimated angles

In second experiment, the gimbal structure translates on a level plane (translational acceleration exists) and the system's tilt are kept constant. Tilt angles calculated by two approaches are shown in Fig. 7.

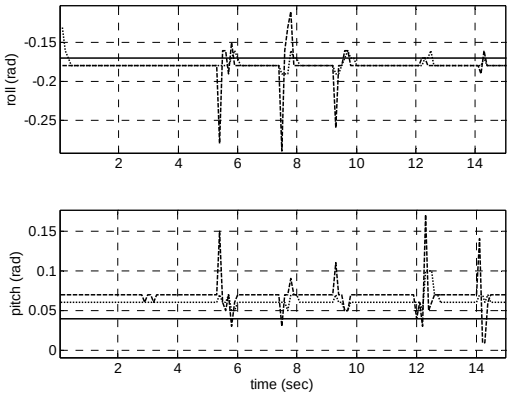

Fig. 7 Tilt angles (roll and pitch) when translational acceleration exists. Solid lines denote true angles, dashed lines angles calculated from accelerometer measurements, and dot lines estimated angles

In this case, error of tilt estimator is much smaller than of accelerometer. Hence, we can conclude that tilt estimator has better performance than accelerometer when the system's translational acceleration is not zero. Because tilt angles are used in tilt compensation of magnetometer data, the improvement in tilt measurement by using tilt estimator instead of accelerometer would reduce tilt compensation error, consequently, heading error.

Compensating for deterministic magnetic noise has been achieved by rotating the system about yaw axis 360 degrees with tilt angles are zeros. While the system is rotating, magnetometer data are sent to computer. Y axis output versus X axis output is plotted in Fig. 8.

We can see that the circle's centre is slightly shifted from coordinate's origin. However, the circle is hardly deformed. It means that the system is affected by hard iron interference while soft iron

interference is very small. To compensate for these interferences, parameters including Xsf, Ysf, Xoff, Yoff have been calculated. In our case, Xsf = 1, Ysf = 1.0056, Xoff = -76.5, Yoff = -13.0734. The result of this compensation is shown in Fig. 8. We can see that after compensation, the circle's centre is coincident with coordinate's origin. It means that the effect of hard iron interference has been removed.

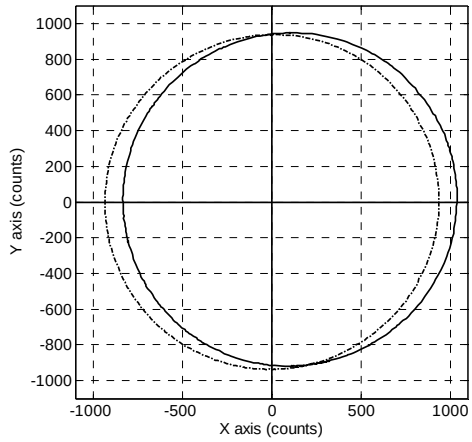

Fig. 8 Magnetometer's Y axis output versus X axis output when the system rotates 360 degrees. Solid line denotes uncompensated data and dashed-dot line compensated data

To verify that our approach can compensate for non-deterministic magnetic interference, heading angle of the system is kept constant while a cell phone passes the system several times. Because the cell phone is not at a fixed position relative to the system, it can be considered as non-deterministic magnetic interference source to the system. Heading angle calculated by using our approach and Caruso's approach[13] are shown in Fig. 9.

We can see that when the cell phone passes the system, heading error of Caruso's approach reaches 0.2 rad while our approach is just 0.05 rad. It has verified that by using our proposed method, heading error due to non-deterministic has decreased remarkably.

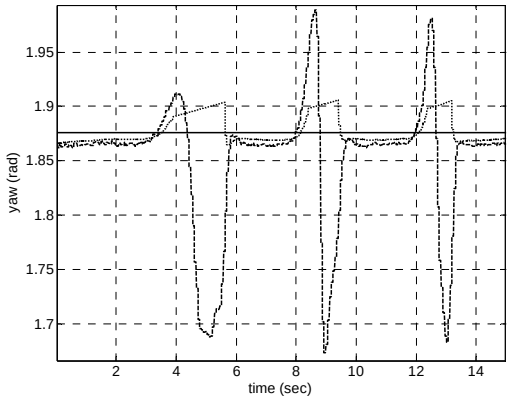

Fig. 9 Heading angle (yaw) when non-deterministic magnetic interference exists. Solid line denote true heading, dashed line heading calculated by Caruso's approach, and dot line heading calculated by proposed approach

5. Conclusions

In this paper, we have presented a tilt and heading estimation system. Three kinds of sensors have been used. Sensors' signals were fused by two linear Kalman filters. The effects of magnetic interferences on heading estimation are considered and compensated. Experimental results have shown that the proposed method have better performance than methods used in previous works. Our tilt and heading estimation system would be used in our ROV project but also can be used for other robots such as flying or climbing ones. Its low-cost, light weight, small size, and reliability make it ideal for many robotic applications.

References

[1] A. J. Baerveldt, R. Klang, "A low-cost and low-weight attitude estimation system for a autonomous helicopter", in Proc. 1997 IEEE Int. Conf. on Intelligent Engineering Systems, Budapest, Hungary, pp. 391-395, 1997.

[2] K. Loffler, M. Gienger, F. Pfeiffer, H. Ulbrich, "Sensors and Control Concept of a Biped Robot", IEEE Trans. on Industrial Electronics, vol. 51, no. 5, pp. 972-980, 2004.

[3] J. Vaganay, M. J. Aldon, A. Fournier, "Mobile robot attitude estimation by fusion of inertial data", in Proc. 1993 IEEE Int. Conf. on Robotics and Automation, Atlanta, GA, USA, vol. 1, pp. 277-282, 1993.

[4] B. Barshan, H. F. Durrant-Whyte, "Inertial navigation systems for mobile robots", IEEE Transactions on Robotics and Automation, vol. 11, no. 3, 1995.

[5] B. Barshan, H. F. Durrant-Whyte, "Evaluation of a solid-state gyroscope for robotics applications", IEEE Transactions on Instrumentation and Measurement, vol. 44, no. 1, 1994.

[6] L. Ojeda, J. Borenstein, "FLEXnav: Fuzzy logic expert rule-based position estimation for mobile robots on rugged terrain", in Proc. 2002 IEEE Int. Conf. on Robotics & Automation, Washington, DC, 2002.

[7] H. Rehbinder, X. Hu, "Drift-free attitude estimation for accelerated rigid bodies", Automatica 40, pp. 653-659, 2004.

[8] D. H. Titterton, J. L. Weston, Strapdown inertial navigation technology, 2nd edition, American Institute of Aeronautics and Astronautics, 2004.

[9] S. Y. Cho, C. G. Park, "Tilt compensation algorithm for 2-axis magnetic compass", Electronics letters, vol. 39, no. 22, 2003.

[10] M. J. Caruso, "Applications of magnetic sensors for low cost compass systems", white paper at Honeywell Inc.

[11] TCM2 Electronic sensor module user's guide, white paper at PNI Corporation.

[12] P. Zarchan, H. Musoff, Fundamentals of kalman filtering: A practical approach, 2nd edition, American Institute of Aeronautics and Astronautics, 2005.

[13] M. J. Caruso, "Applications of magnetoresistive sensors in navigation systems" in white paper at Honeywell Inc.

[14] D. Jurman, M. Jankovec, R. Kamnik, M. Topic, "Calibration and data fusion solution for the miniature attitude and heading reference system", Sensors and Actuators A 138, pp. 411-420, 2007.

Author Profile

Yun-Su HA

was born in Kyeongju, Korea, in 1962. He received B.E. and M.S. degrees from Korea Maritime University, Busan, Korea, in 1986 and 1990, respectively. And also he received Ph.D. degree in electronics and information sciences from University of Tsukuba, Ibaraki, Japan, in 1996. Since 1996 he has been work at Korea Maritime University, and is now a professor and leads the Intelligent Robot Lab.
His major research field is mobile robot control and sensor data fusion.

Thanh-Hoan Ngo

was born in Ho Chi Minh city, Vietnam in 1983. He received B.E. degree from Ho Chi Minh city University of Technology, Vietnam in 2006 and received M.S. degree from Korea Maritime University, Busan, Korea, in 2008.